The low-bias conducting mechanism of single-molecule junctions constructed with methylsulfide linker groups and gold electrodes

Minglang Wang, Yongfeng Wang, Stefano Sanvito, and Shimin Hou

Articles you may be interested in

Temperature dependent tunneling conductance of single molecule junctions
The Journal of Chemical Physics **146**, 092311 (2017); 10.1063/1.4973318

Uncovering hierarchical data structure in single molecule transport
The Journal of Chemical Physics **146**, 092321 (2017); 10.1063/1.4974937

Enhancing the conductivity of molecular electronic devices
The Journal of Chemical Physics **146**, 092310 (2016); 10.1063/1.4972992

Adsorption and charge transfer interactions of bi-isonicotinic acid on Ag(111)
The Journal of Chemical Physics **147**, 054703 (2017); 10.1063/1.4996746

Destructive quantum interference in electron transport: A reconciliation of the molecular orbital and the atomic orbital perspective
The Journal of Chemical Physics **146**, 092308 (2016); 10.1063/1.4972572

Transport mirages in single-molecule devices
The Journal of Chemical Physics **146**, 092330 (2017); 10.1063/1.4975767

AIP | The Journal of Chemical Physics

PERSPECTIVES

The low-bias conducting mechanism of single-molecule junctions constructed with methylsulfide linker groups and gold electrodes

Minglang Wang,[1] Yongfeng Wang,[1,2] Stefano Sanvito,[3] and Shimin Hou[1,2,a)]

[1]*Key Laboratory for the Physics and Chemistry of Nanodevices, Department of Electronics, Peking University, Beijing 100871, China*
[2]*Beida Information Research (BIR), Tianjin 300457, China*
[3]*School of Physics, AMBER and CRANN Institute, Trinity College, Dublin 2, Ireland*

The atomic structure and electronic transport properties of two types of molecular junctions, in which a series of saturated and conjugated molecules are symmetrically connected to gold electrodes through methylsulfide groups, are investigated using the non-equilibrium Green's function formalism combined with density functional theory. Our calculations show that the low-bias junction conductance is determined by the electronic tunneling between the two Au–S donor-acceptor bonds formed at the molecule-electrode interfaces. For alkanes with 4, 6, and 8 carbon atoms in the chain, the Au–S bonds moderately couple with the σ-type frontier molecular orbitals of the alkane backbone and thus prefer to be coplanar with the alkane backbone in the junction. This results in an exponential decrease of the junction conductance as a function of the number of methylene groups. In contrast, the Au–S bonds couple strongly with the π-type orbitals of the 1,4'-bis(methylsulfide)benzene and 4,4'-bis(methylsulfide)biphenyl molecules and thus tend to be perpendicular to the neighboring benzene rings, leading to the rather large junction conductance. Our findings contribute to the understanding of the low-bias conducting mechanism and facilitate the design of molecular electronic devices with methylsulfide groups and gold electrodes. *Published by AIP Publishing.* [http://dx.doi.org/10.1063/1.4996745]

I. INTRODUCTION

Exploring the structure-property relationship of electronic devices using single molecules as the active component is the cutting edge research in molecular electronics.[1] Single-molecule devices also provide an ideal platform for the investigation of basic quantum transport concepts. When a single molecule is wired between two metal electrodes, the molecule-electrode contacts that are formed by the metal electrodes and the linker groups flanked at the two ends of the central molecule have profound effects on the electronic transport properties of molecular junctions.[2] Besides the widely used thiol, pyridine, and amine groups,[3–5] methylsulfide (SMe) is often employed as the linker bonded to gold electrodes.[6–33] For example, with the Au–SMe bonds single-molecule diodes with rectification ratios higher than 200 at voltages as low as 370 mV were fabricated in an ionic solution.[27] Furthermore, single-molecule switches operating through a stereo-electronic effect were first realized in oligosilane molecules connected to gold electrodes through SMe linkers.[25] It is generally accepted that for thiol groups the Au–S covalent bonds are formed at the molecule-electrode interfaces while pyridine, amine, and methylsulfide groups form donor-acceptor bonds with undercoordinated gold atoms on the electrode surface because of the lone pairs in the corresponding N or S atom. Unfortunately, up to now the detailed atomic structures of the

molecule-electrode contacts are still not clearly known and thus out of control in experiments. In contrast, computer simulations can take into account the atomic details of molecular junctions and improve our understanding of their electronic transport properties. Although many theoretical investigations have been devoted to exploring the conducting mechanism of molecular junctions constructed using the thiol, pyridine, and amine groups,[34–40] only a few theoretical studies focus on the intrinsic properties of the molecule-electrode interfaces formed by the Au–SMe bonds.[31,41] Therefore, it is highly desirable to carry out first-principles calculations on representative molecular junctions constructed with the Au–SMe bonds.

Here we investigate the structural and electronic transport properties of a series of saturated and conjugated molecules with SMe groups at the two ends. This is realized by employing the non-equilibrium Green's function formalism (NEGF) combined with density function theory (DFT), i.e., the NEGF + DFT approach.[42–50] Our calculations show that the Au–S donor-acceptor bonds formed by the SMe group with the Au adatom on the electrode surface play an important role in the low-bias junction conductance. When the Au–S bonds are nearly coplanar with the alkane backbones or perpendicular to the adjacent benzene rings in the Au-molecule-Au junctions, the calculated values of the low-bias junction conductance are in semi-quantitative or even quantitative agreement with the measured values. In this case the transport is dominated by the highest occupied molecular orbital (HOMO) and the HOMO-1 orbital of the central molecule.

a)Author to whom correspondence should be addressed: smhou@pku.edu.cn

II. CALCULATION METHOD

We employ the SIESTA software package to investigate the atomic and electronic structures of Au-molecule-Au molecular junctions and the SMEAGOL code to study their electronic transport properties.[49–51] SIESTA is an efficient DFT package for numerical simulations of large system with affordable resources, in which the wave functions of valence electrons are expanded over a finite-range numerical basis set and the core electrons are described by norm-conserving Troullier-Martins pseudopotentials.[51,52] While a double-zeta plus polarization (DZP) basis set is used for H, C, and S atoms, two different types of basis functions are used for Au, respectively, in the bulk and at the surface. In more detail, a DZP basis is used for the Au surface atoms, while a single-zeta plus polarization (SZP) basis is used for the bulk. The exchange-correlation functional is treated at the level of the generalized gradient approximation (GGA) within the Perdew-Burke-Ernzerhof (PBE) formulation.[53] Geometry optimization is performed by standard conjugate gradient until all the atomic forces are smaller than 0.03 eV Å^{-1}.

SMEAGOL is a practical implementation of the NEGF + DFT approach, which uses SIESTA as the DFT platform.[49,50] Periodic boundary conditions are applied in the plane transverse to the transport direction, while the unit cell of the extended molecule includes the central molecule and ten atomic layers of the gold electrodes with a (3 × 3) supercell. An equivalent cutoff of 200.0 Ry is taken for the real space grid integration. The charge density is integrated over 24 energy points along the semi-circle, 24 points along the line in the complex plane, while 24 poles are used for the Fermi function (the electronic temperature is 25 meV). The transmission coefficient $T(E)$ of the molecular junction is evaluated as

$$T(E) = \frac{1}{\Omega_{2DBZ}} \int_{2DBZ} T(\vec{k}; E) d\vec{k}, \tag{1}$$

where Ω_{2DBZ} is the area of the two-dimensional Brillouin zone (2DBZ) in the transverse directions. The k-dependent transmission coefficient $T(\vec{k}; E)$ is obtained as

$$T(\vec{k}; E) = Tr[\Gamma_L G_M^R \Gamma_R G_M^{R+}], \tag{2}$$

where G_M^R is the retarded Green's function matrix of the extended molecule and Γ_L (Γ_R) is the broadening function matrix describing the interaction of the extended molecule with the left-hand (right-hand) side electrode. Here, we calculate the transmission coefficient by sampling 4 × 4 k-points in the transverse 2DBZ.

III. RESULTS AND DISCUSSION

We start our studies from the investigation of the atomic structure and the electronic transport properties of alkanes with 4, 6, and 8 methylene groups terminated by two SMe groups. The ground state of the isolated 1,4-bis(methylsulfide)butane (SMe–C4–SMe) molecule has the two carbon atoms in the SMe groups optimized to be out of the plane defined by the four carbon atoms of the butane backbone [Fig. 1(a)], which is characterized by the dihedral angle ∠C(SMe)–S–C–C = 71.6°. Both the HOMO and HOMO-1 orbitals are dominated by
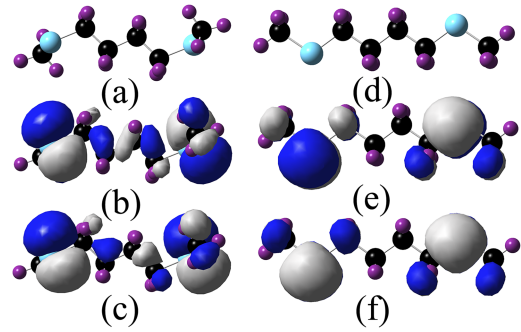

FIG. 1. The optimized atomic structure (a), HOMO (b), and HOMO-1 (c) of the SMe–C4–SMe molecule with the two carbon atoms in the SMe groups out of the plane of the butane backbone; the optimized atomic structure (d), HOMO (e), and HOMO-1 (f) of the SMe–C4–SMe molecule with the two carbon atoms in the SMe groups coplanar with the butane backbone. Purple, black, and cyan spheres are, respectively, hydrogen, carbon, and sulfur atoms.

the occupied S 3p atomic orbitals in the two SMe groups. Since these two S 3p atomic orbitals are coplanar with the four carbon atoms of the butane backbone, they are coupled across the butane backbone resulting in an energy splitting of ~130 meV between the HOMO and HOMO-1 orbitals. It should be noted that the SMe–C4–SMe molecule with the two carbon atoms in the SMe groups coplanar with the butane backbone (the dihedral angle ∠C(SMe)–S–C–C = 180°) is also a local minimum, and its total energy is only 26 meV higher than that of the ground state geometry. In contrast, the corresponding HOMO and HOMO-1 orbitals are almost degenerate and are both composed of two localized S 3p atomic orbitals perpendicular to the plane of the butane backbone [see Figs. 1(e) and 1(f)]. Due to the rather small energy difference, the SMe–C4–SMe molecule with both these two conformations may appear in Au–SMe–C4–SMe–Au molecular junctions fabricated with the scanning tunneling microscopy break junction (STM-BJ) method at room temperature.[6,10,28]

Figure 2(a) shows the optimized atomic structure of the Au–SMe–C4–SMe–Au molecular junction, in which the two SMe groups are assumed to bind with the Au adatoms of the Au(111) surface. In order to find the equilibrium structure, we systematically vary the separation between the two gold electrodes and optimize the positions of the SMe–C4–SMe molecule, gold adatoms, and those at the electrode surfaces until the total energy reaches a local minimum. The bond length of the Au–S donor-acceptor bonds is optimized to be 2.47 Å, and the dihedral angles ∠Au–S–C–C and ∠C(SMe)–S–C–C are, respectively, optimized to be ~176° and ~82°. The corresponding equilibrium transmission spectrum is presented in Fig. 2(b). Clearly, there are two transmission peaks around the Fermi level, one peak centered at −1.77 eV and the other centered at 2.64 eV. Because these two transmission peaks decay rapidly towards the Fermi level, the transmission coefficient at the Fermi level is calculated to be 2.8 × 10^{-3}, which is consistent with the experimental value of 1.4 × 10^{-3}.[6,10] A deep understanding can be obtained by projecting the transmission onto the frontier molecular orbitals of the SMe–C4–SMe molecule [Fig. 2(c)].[54] The transmission peak at −1.77 eV and the transmission around the Fermi level are dominated by the HOMO and HOMO-1 orbitals of the SMe–C4–SMe molecule. By comparing with the local density
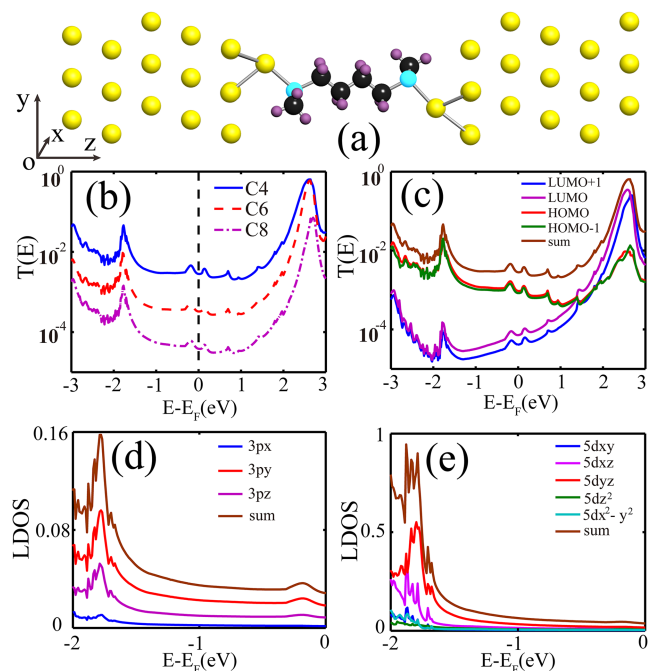
FIG. 2. The atomic structure and electronic transport properties of the Au–SMe–C$_4$–SMe–Au molecule junction with the Au–S bonds nearly coplanar with the butane backbone: (a) the optimized atomic structure, (b) the equilibrium transmission spectrum, (c) the transmission spectrum projected onto frontier molecular orbitals of SMe–C$_4$–SMe, (d) the LDOS projected onto the S 3p atomic orbitals, and (e) the LDOS projected onto the 5d orbitals of the Au adatom. Purple, black, cyan, and yellow color spheres in (a) are, respectively, hydrogen, carbon, sulfur, and gold atoms. For comparison, the equilibrium transmission spectra of the Au–SMe–C$_6$–SMe–Au and Au–SMe–C$_8$–SMe–Au molecular junctions are also given in (b).
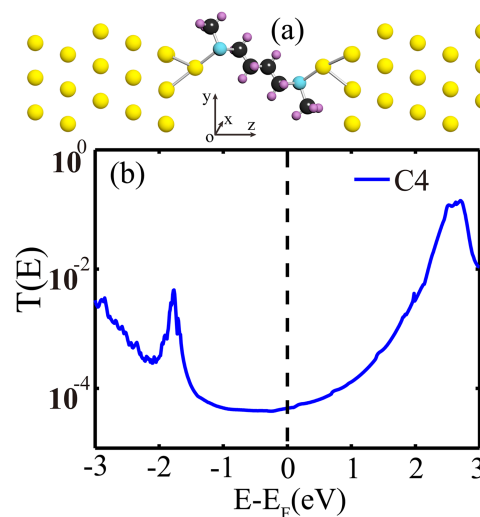

FIG. 3. The optimized atomic structure (a) and the equilibrium transmission spectrum (b) of the Au–SMe–C$_4$–SMe–Au molecular junction with the Au–S bonds out of the plane of the butane backbone.

of states (LDOS) projected onto the atomic orbitals of the sulfur atoms in the SMe groups and the Au adatoms [Figs. 2(d) and 2(e)], we establish that the HOMO and HOMO-1 orbitals of the SMe–C$_4$–SMe molecule are mainly composed of the S 3p$_y$ atomic orbitals when the butane backbone is placed along the yOz plane in the junction. This in turn couples to the Au 5d$_{yz}$ atomic orbital contributing to the transmission peak centered at −1.77 eV and determines the transmission around the Fermi level.

In contrast, when the two carbon atoms in the SMe groups are nearly coplanar with the butane backbone in the Au–SMe–C$_4$–SMe–Au junction, which is characterized by the dihedral angles ∠Au–S–C–C = 87° and ∠C(SMe)–S–C–C = 170° [Fig. 3(a)], the junction transmission is reduced significantly. As it can be seen in Fig. 3(b), the transmission coefficient at the Fermi level is calculated to be 4.7 × 10^{-5} that is much less than the measured value, despite the fact that two transmission peaks appear, respectively, at −1.77 eV and 2.63 eV. The much-reduced transmission should be ascribed to the more localized HOMO and HOMO-1 orbitals of the SMe–C$_4$–SMe molecule in this conformation [Figs. 1(e) and 1(f)], since the electronic coupling of the Au–S interfaces should not be changed too much due to the very similar Au–S donor-acceptor bond lengths (2.49 Å). Therefore, the most probable molecule-electrode interfaces in Au–SMe–C$_4$–SMe–Au molecule junctions are formed by the Au–S donor-acceptor bonds that are nearly coplanar with the butane backbone.

Then we calculate the transport properties of 1,6-bis(methylsulfide)hexane (SMe–C$_6$–SMe) and 1,8-bis (methylsulfide)octane (SMe–C$_8$–SMe) molecules contacted with gold electrodes [Fig. 2(b)]. With the optimized Au–S bond length of 2.47 Å and the dihedral angle ∠Au–S–C–C approaching 180°, the transmission coefficients at the Fermi level are calculated to be 3.3 × 10^{-4} for Au–SMe–C$_6$–SMe–Au and 3.8 × 10^{-5} for Au–SMe–C$_8$–SMe–Au junctions, both in excellent agreement with the corresponding measured values of 3.1 × 10^{-4} and 3.9 × 10^{-5}.[6,26] By using the same analysis carried out for the Au–SMe–C$_4$–SMe–Au junction, we can confirm that the interaction between the Au 5d$_{yz}$ and S 3p$_y$ atomic orbitals dominates the transmission peak centered at −1.77 eV and the transmission around the Fermi level for both Au–SMe–C$_6$–SMe–Au and Au–SMe–C$_8$–SMe–Au. Therefore, the low-bias conductance of the Au–SMe–C$_n$–SMe–Au molecular junctions mainly originates from the electronic tunneling between the two localized Au–S donor-acceptor bonds that are mediated by the central alkane chains, where n is the number of carbon atoms in the chain. The longer the alkane chains and the larger the dihedral angle between the Au–S bond and the alkane backbone, the lower the junction conductance. This tunneling mechanism of conduction is also corroborated by the length-dependence of the junction conductance. For these three molecular junctions, the conductance decreases exponentially with the increase of the length of the central alkanes, which can be described with the relation $G \sim \exp(-\beta n)$. Here, G is the junction conductance, and β is the decay constant. The decay constant β is determined to be 1.0 per methylene group, in good agreement with the measured value of 0.94 ± 0.05.[28]

Next we turn to investigate the electronic transport properties of conjugated molecules terminated with one SMe group at each end, and choose 1,4'-bis(methylsulfide)benzene (SMe–Ph–SMe) and 4,4'-bis(methylsulfide)biphenyl (SMe–Ph$_2$–SMe) as the representative cases. Different from the SMe–C$_n$–SMe alkanes investigated above, in the ground state the two carbon atoms in the SMe groups are found to be
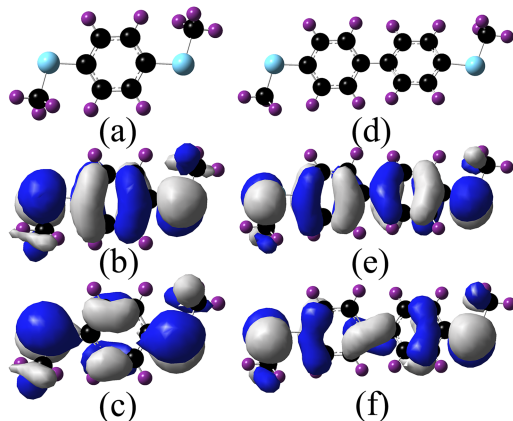
FIG. 4. The optimized atomic structure (a), HOMO (b), and HOMO-1 (c) of the SMe–Ph–SMe molecule; the optimized atomic structure (d), HOMO (e), and HOMO-1 (f) of the SMe–Ph$_2$–SMe molecule.

coplanar with the benzene backbone for the isolated SMe–Ph–SMe molecule [Fig. 4(a)]. Thus, the S 3p lone pairs in the two SMe groups can have a strong coupling with the π-type orbitals of the benzene backbone. The S–C(benzene) bond lengths are optimized to be 1.777 Å shorter than the S–C(methylene) bond with a length of 1.836 Å in the SMe–C$_4$–SMe molecule, further strengthening the coupling between the S 3p lone pairs and the π-type benzene orbitals. As shown in Figs. 4(b) and 4(c), the HOMO and HOMO-1 orbitals of the SMe–Ph–SMe molecule are both π-type delocalized along the entire molecule including the benzene backbone and the two sulfur atoms of the SMe groups, and their energy splitting is about 1.15 eV. Similar atomic and electronic structures are obtained for the isolated SMe–Ph$_2$–SMe molecule [Figs. 4(d)–4(f)]. The carbon atoms in the two SMe groups are coplanar with their neighboring benzene rings; the HOMO and HOMO-1 orbitals are also π-type but with a smaller energy splitting of 0.58 eV.

For the Au–SMe–Ph–SMe–Au molecular junction [Fig. 5(a)], the two SMe groups are also assumed to bind with the Au adatom of the Au(111) surface with an optimized Au–S bond length of 2.51 Å and a dihedral angle ∠Au–S–C–C
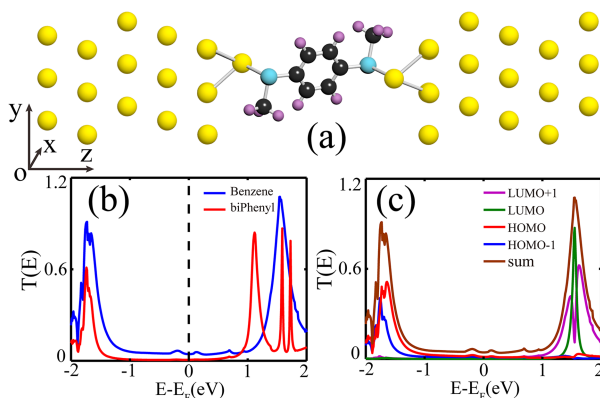

FIG. 5. The atomic structure and electronic transport properties of the Au–SMe–Ph–SMe–Au molecule junction: (a) the optimized atomic structure, (b) the equilibrium transmission spectrum, and (c) the transmission spectrum projected onto frontier molecular orbitals of SMe–Ph–SMe. For comparison, the equilibrium transmission spectra of the Au–SMe–Ph$_2$–SMe–Au molecular junctions are also given in (b).

of 96°. The equilibrium transmission spectrum is shown in Fig. 5(b). The first transmission peak below the Fermi level is located at −1.73 eV, indicating that the Au–S bonding is almost the same as that in the Au–SMe–C$_n$–SMe–Au junctions. In contrast, the first transmission peak above the Fermi level is shifted downwards in energy to 1.55 eV due to the much reduced HOMO-LUMO gap of the SMe–Ph–SMe molecule. Here, LUMO is the acronym of the lowest unoccupied molecular orbital. By projecting the transmission spectrum onto the frontier molecular orbitals of SMe–Ph–SMe [Fig. 5(c)], we can deduce that the transmission peak at −1.73 eV and the transmission around the Fermi level are dominated by the HOMO and HOMO-1 orbitals. The transmission coefficient at the Fermi level is calculated to be 4.3×10^{-2}, slightly larger than the actual measured value of $(0.9 \pm 0.05) \times 10^{-2}$.[8] Considering that GGA functionals like PBE always underestimate the HOMO position (too high in energy) and thus overestimate the low-bias junction conductance,[55] this result is quite acceptable. Since the π-type HOMO and HOMO-1 orbitals of SMe–Ph–SMe provide a better coupling between the Au–S donor-acceptor bonds, the Au–SMe–Ph–SMe–Au junction is more conducting than the Au–SMe–C$_4$–SMe–Au one. With the optimized Au–S bond length of 2.51 Å and the dihedral angle of ∠Au–S–C–C = 66°, the calculated transmission spectrum of the Au–SMe–Ph$_2$–SMe–Au junction is presented in Fig. 5(b). When compared to that of the Au–SMe–Ph–SMe–Au junction, the first transmission peak below the Fermi level does not change its position but presents a reduced amplitude. The transmission coefficient at the Fermi level is only 6.2×10^{-3}, in good agreement with the measured value of 2×10^{-3},[17] though the first transmission peak above the Fermi level is further shifted downwards to 1.12 eV. The transmission around the Fermi level is still mainly contributed by the HOMO and HOMO-1 orbitals of the SMe–Ph$_2$–SMe molecule. Although the SMe–Ph$_2$–SMe molecule has a higher conjugation than that of SMe–Ph–SMe and thus has a smaller HOMO-LUMO gap, the dihedral angle (∼36°) between two benzene rings reduces the efficiency of the electronic coupling between the S 3p lone pairs of the two SMe groups leading to the lower conductance of the Au–SMe–Ph$_2$–SMe–Au junction.

Transport calculations have also been performed for junctions under moderate compressive and tensile strain, obtained by changing the distance between the electrodes up to ±0.5 Å from the equilibrium position. In all cases, although the relaxation gives alterations in the details of the bonding structure, we find that the transmission remains almost unchanged, indicating that the SMe anchoring group makes the transport stable against geometry fluctuations.

IV. CONCLUSION

We have investigated the atomic structures and electronic transport properties of molecular junctions employing the NEGF + DFT approach, in which the alkanes and aromatic molecules are connected to gold electrodes through SMe linkers. Our calculations show that electronic tunneling between the Au–S bonding states at the two molecule-electrode interfaces dominates the low-bias junction conductance, which is

mediated by the central aliphatic and aromatic molecules. Since the frontier molecular orbitals of the central aliphatic and aromatic molecules are, respectively, σ-type and π-type, the Au–S donor-acceptor bonds tend to be parallel to the alkane backbones or be perpendicular to the neighboring benzene rings, thus enabling a better electronic coupling between the Au–S bonding states. This is also the main reason for the low-bias conductance of the Au–SMe–Ph–SMe–Au and Au–SMe–Ph$_2$–SMe–Au junctions to be much larger than those of the Au–SMe–C$_n$–SMe–Au junctions with a similar molecular length. Our findings are helpful in the development and application of methyl sulfide linker groups in future molecular electronic devices.

ACKNOWLEDGMENTS

[1] D. Xiang, X. Guo, and T. Lee, Chem. Rev. **116**, 4318 (2016).
[2] E. Leary, A. La Rosa, M. Teresa González, G. Rubio-Bollinger, N. Agraït, and N. Marth, Chem. Soc. Rev. **44**, 920 (2015).
[3] M. A. Reed, C. Zhou, C. J. Muller, T. P. Burgin, and J. M. Tour, Science **278**, 252 (1997).
[4] B. Q. Xu and N. J. Tao, Science **301**, 1221 (2003).
[5] L. Venkataraman, J. E. Klare, C. Nuckolls, M. S. Hybertsen, and M. L. Steigerwald, Nature **442**, 904 (2006).
[6] Y. S. Park, A. C. Whalley, M. Kamenetska, M. L. Steigerwald, M. S. Hybertsen, C. Nuckolls, and L. Venkataraman, J. Am. Chem. Soc. **129**, 15768 (2007).
[7] M. Kamenetska, M. Koentopp, A. C. Whalley, Y. S. Park, M. L. Steigerwald, C. Nuckolls, M. S. Hybertsen, and L. Venkataraman, Phys. Rev. Lett. **102**, 126803 (2009).
[8] Y. S. Park, J. R. Widawsky, M. Kamenetska, M. L. Steigerwald, M. S. Hybertsen, C. Nuckolls, and L. Venkataraman, J. Am. Chem. Soc. **131**, 10820 (2009).
[9] J. S. Meisner, M. Kamenetska, M. Krikorian, M. L. Steigerwald, L. Venkataraman, and C. Nuckolls, Nano Lett. **11**, 1575 (2011).
[10] M. Frei, S. V. Aradhya, M. S. hybertsen, and L. Venkataraman, J. Am. Chem. Soc. **134**, 4003 (2012).
[11] R. S. Klausen, J. R. Widawsky, M. L. Steigerwald, L. Venkataraman, and C. Nuckolls, J. Am. Chem. Soc. **134**, 4541 (2012).
[12] S. V. Aradhya, J. S. Meisner, M. Krikorian, S. Ahn, R. Parameswaran, M. L. Steigerwald, C. Nuckolls, and L. Venkataraman, Nano Lett. **12**, 1643 (2012).
[13] S. Ahn, S. V. Aradhya, R. S. Klausen, B. Capozzi, X. Roy, M. L. Steigerwald, C. Nuckolls, and L. Venkataraman, Phys. Chem. Chem. Phys. **14**, 13841 (2012).
[14] H. Vazquez, R. Skouta, S. Schneebeli, M. Kamenetska, R. Breslow, L. Venkataraman, and M. S. Hybertsen, Nat. Nanotechnol. **7**, 663 (2012).
[15] X. Roy, C. L. Schenck, S. Ahn, R. A. Lalancette, L. Venkataraman, C. Nuckolls, and M. L. Steigerwald, Angew. Chem., Int. Ed. **51**, 12473 (2012).
[16] J. S. Meisner, S. Ahn, S. V. Aradhya, M. Krikorian, R. Parameswaran, M. L. Steigerwald, L. Venkataraman, and C. Nuckolls, J. Am. Chem. Soc. **134**, 20440 (2012).
[17] E. J. Dell, B. Capozzi, K. H. Dubay, T. C. Berkelbach, J. R. Moreno, D. R. Reichman, L. Venkataraman, and L. M. Campos, J. Am. Chem. Soc. **135**, 11724 (2013).
[18] A. Batra, P. Darancet, Q. Chen, J. S. Meisner, J. R. Widawsky, J. B. Neaton, C. Nuckolls, and L. Venkataraman, Nano Lett. **13**, 6233 (2013).
[19] T. A. Su, J. R. Widawsky, H. Li, R. S. Klausen, J. L. Leighton, M. L. Steigerwald, L. Venkataraman, and C. Nuckolls, J. Am. Chem. Soc. **135**, 18331 (2013).
[20] A. Batra, J. S. Meisner, P. Darancet, Q. Chen, M. L. Steigerwald, C. Nuckolls, and L. Venkataraman, Faraday Discuss. **174**, 79 (2014).
[21] S. V. Aradhya, A. Nielsen, M. S. Hybertsen, and L. venkataraman, ACS Nano **8**, 7522 (2014).
[22] B. Capozzi, E. J. Dell, T. C. Berkelbach, D. R. Reichman, L. Venkataraman, and L. M. Campos, J. Am. Chem. Soc. **136**, 10486 (2014).
[23] E. J. Dell, B. Capozzi, J. Xia, L. venkataraman, and L. M. Campos, Nat. Chem. **7**, 209 (2015).
[24] H. Li, T. A. Su, V. Zhang, M. L. Steigerwald, C. Nuckolls, and L. Venkataraman, J. Am. Chem. Soc. **137**, 5028 (2015).
[25] T. A. Su, H. Li, M. L. Steigerwald, L. Venkataraman, and C. Nuckolls, Nat. Chem. **7**, 215 (2015).
[26] O. Adak, E. Rosenthal, J. Meisner, E. F. Andrade, A. N. Pasupathy, C. Nuckolls, M. S. Hybersen, and L. Venkataraman, Nano Lett. **15**, 4143 (2015).
[27] B. Capozzi, J. Xia, O. Adak, E. J. Dell, Z. Liu, J. C. Taylor, J. B. Neaton, L. M. Campos, and L. venkataraman, Nat. Nanotechnol. **10**, 522 (2015).
[28] T. A. Su, H. Li, V. Zhang, M. Neupane, A. Batra, R. S. Klausen, B. Kumar, M. L. Steigerwald, L. Venkataraman, and C. Nuckolls, J. Am. Chem. Soc. **137**, 12400 (2015).
[29] M. S. Hybertsen and L. Venkataraman, Acc. Chem. Res. **49**, 452 (2016).
[30] B. Capozzi, J. Z. Low, J. Xia, Z. Liu, J. B. Neaton, L. M. Campos, and L. Venkataraman, Nano Lett. **16**, 3949 (2016).
[31] H. Li, M. H. Garner, Z. Shangguan, Q. Zheng, T. A. Su, M. Neupane, P. Li, A. Velian, M. L. Steigerwald, S. Xiao, C. Nuckolls, G. C. Solomon, and L. Venkataraman, Chem. Sci. **7**, 5657 (2016).
[32] T. A. Su, H. Li, R. S. Klausen, J. R. Widawsky, A. Batra, M. L. Steigerwald, L. Venkataraman, and C. Nuckolls, J. Am. Chem. Soc. **138**, 7791 (2016).
[33] N. T. Kim, H. Li, L. Venkataraman, and J. L. Leighton, J. Am. Chem. Soc. **138**, 11505 (2016).
[34] Y. Q. Xue and M. A. Ratner, Phys. Rev. B **68**, 115406 (2003).
[35] C. Li, I. Pobelov, T. Wandlowski, A. Bagrets, A. Arnold, and F. Evers, J. Am. Chem. Soc. **130**, 318 (2008).
[36] S. Hou, J. Zhang, R. Li, J. Ning, R. Han, Z. Shen, X. Zhao, Z. Xue, and Q. Wu, Nanotechnology **16**, 239 (2004).
[37] J. Ning, R. Li, X. Shen, Z. Qian, S. Hou, A. R. Rocha, and S. Sanvito, Nanotechnology **18**, 345203 (2007).
[38] S. Y. Quek, M. Kamenetska, M. L. Steigerwald, H. J. Choi, S. G. Louie, M. S. Hybertsen, J. B. Neaton, and L. Venkataraman, Nat. Nanotechnol. **4**, 230 (2009).
[39] M. Strange, C. Rostgaard, H. Hakkinen, and K. S. Thygesen, Phys. Rev. B **83**, 115108 (2011).
[40] S. Y. Quek and K. H. Khoo, Acc. Chem. Res. **47**, 3250 (2014).
[41] X. Y. Feng, Z. Li, and J. Yang, J. Phys. Chem. C **113**, 21911 (2009).
[42] Y. Meir and N. S. Wingreen, Phys. Rev. Lett. **68**, 2512 (1992).
[43] P. Hohenberg and W. Kohn, Phys. Rev. **136**, B864 (1964).
[44] W. Kohn and L. J. Sham, Phys. Rev. **140**, A1133 (1965).
[45] Y. Xue, S. Datta, and M. A. Ratner, Chem. Phys. **281**, 151 (2002).
[46] M. Brandbyge, J.-L. Mozos, P. Ordejón, J. Taylor, and K. Stokbro, Phys. Rev. B **65**, 165401 (2002).
[47] J. Zhang, S. Hou, R. Li, Z. Qian, R. Han, Z. Shen, X. Zhao, and Z. Xue, Nanotechnology **16**, 3057 (2005).
[48] R. Li, J. Zhang, S. Hou, Z. Qian, Z. Shen, X. Zhao, and Z. Xue, Chem. Phys. **336**, 127 (2007).
[49] A. R. Rocha, V. M. García-Suárez, S. W. Bailey, C. J. Lambert, J. Ferrer, and S. Sanvito, Nat. Mater. **4**, 335 (2005).
[50] A. R. Rocha, V. M. García-Suárez, S. Bailey, C. Lambert, J. Ferrer, and S. Sanvito, Phys. Rev. B **73**, 085414 (2006).
[51] J. M. Soler, E. Artacho, J. D. Gale, A. García, J. Junquera, P. Ordejón, and D. Sánchez-Portal, J. Phys.: Condens. Matter **14**, 2745 (2002).
[52] N. Troullier and J. L. Martins, Phys. Rev. B **43**, 1993 (1991).
[53] J. P. Perdew, K. Burke, and M. Ernzerhof, Phys. Rev. Lett. **77**, 3865 (1996).
[54] R. Li, S. Hou, J. Zhang, Z. Qian, Z. Shen, and X. Zhao, J. Chem. Phys. **125**, 194113 (2006).
[55] C. Toher and S. Sanvito, Phys. Rev. Lett. **99**, 056801 (2007).